LA-UR-14-23276
Approved for public release; distribution is unlimited.

Title: Analysis of Differential Die Away Instrument Simulated Performance Using Boiling Water Reactor Spent Fuel Assemblies

Author(s): Henzl, Vladimir
Trellue, Holly R.
Fischer, Noah A.
Weldon, Robert A. Jr.

Intended for: Report

Issued: 2014-05-09

Analysis of Differential Die Away Instrument Simulated Performance Using Boiling Water Reactor Spent Fuel Assemblies

Vladimir Henzl, Holly Trellue, Noah Fischer, Robert Weldon

Introduction

As part of evaluating the performance of various Non-Destructive Assay (NDA) instruments measuring the plutonium content and other information about spent nuclear fuel, the Next Generation of Safeguards Initiative (NGSI) Spent Fuel (SF) Project generated spent fuel libraries containing the composition of spent fuel assemblies originating from various reactors, initial enrichments (IE), burnups (BU), and cooling times (CT) [1,2]. Spent Fuel Library (SFL) number 5 (SFL5), representing Boiling Water Reactor (BWR) assemblies, was created as part of a "Gentleman's Agreement" with Sweden to examine if the Differential Die Away (DDA) instrument performs similarly for BWR assemblies as for the Pressurized Water Reactor (PWR) ones. The difference between PWRs and BWRs is that BWRs have a large axial variation in moderator density because it is in the form of water at the bottom of the reactor but turns into steam as it gets warmer at the top of the reactor; thus, more plutonium builds up at the bottom of each assembly than at the top. In a PWR, the moderator density varies slightly from the bottom to the top, but since it is pressurized, the changes are not as significant with respect to the burnup and plutonium distributions. BWR assemblies are also typically smaller than PWR ones, which could affect detector performance. Since Sweden has both PWR and BWR assemblies, it is anticipated that we will be deploying the DDA instrument to measure both spent fuel assembly (SFA) types.

Methodology

The MCNP input files for the BWR assemblies were generated by the code LWRGen, which was initially designed and implemented with C/C++ to generate full PWR cores with fresh fuel but expanded to include BWR assemblies [3]. Options in the generation input file allow for variable assembly sizes and zoning of fuel into equal volume axial and radial zones, each with their own material compositions, so that a desired fidelity may be achieved. The fresh fuel composition is determined by specifying the density and enrichment values, and includes both ^{234}U and ^{235}U isotopes. Fuel pin geometry is generated by specifying the pellet radius, pin pitch and height; gap radius and height; and values for the cladding radius, top, and bottom. Guide tubes are generated by specifying their inner and outer radii, and placed within the assemblies by specifying their locations within an assembly fuel mapping grid. The assembly locations are then specified in the core mapping grid, and the inner core radius is then determined from the outer most fuel pin unless the user inputs a specific value. Temperature parameters for the fuel, cladding, and water allow for the user to specify the values that should be used during the simulation. For BWRs, channel parameters were implemented for specifying the distance from an edge fuel pin to the box, the box's thickness, and distance to the center of a control blade. Control blades are determined by specifying the inner and outer width of the blade; the inner and outer radii of the control pins within the blade; control pin pitch within the blade; a spacing parameter determining the extent of the blade; and how many pins are within each extending section of a blade. The blades were created as quadrant sections so that they can be used in lattices and placed in the core using a blade mapping grid. Axial zoning of the moderator was also added to correctly model the variation in the moderator density with height, and allows the user to specify the densities for each region. Reflectivity options were also updated for infinitely reflective assemblies to allow for greater fidelity in modeling a single fuel assembly.

Finally, water wings and a water channel were implemented to create the additional BWR geometry shown in Figure 1, which represents a SVEA 96 assembly from Sweden. The water channel size is determined by a single parameter while the wings use three: the distance from the channel, the width of

the wing, and the length of the wing. One additional parameter is used for specifying the thickness of the zircalloy enclosing the wings and channel. The assembly map was also updated to allow for the pins to be split into four separate grids, and an option for specifying moderator regions within the assembly without guide tubes was included. Gadolinium rods were also added for more accurate modeling of real assemblies.

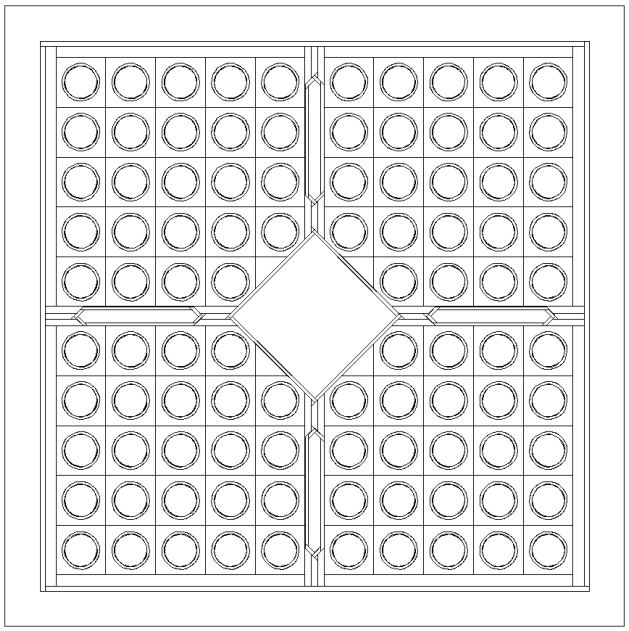

Fig. 1: MCNP Plot showing boxed 4x(5x5) BWR assembly with water wings and a water channel. The four center pins were removed by specifying them as moderator, allowing for the moderator density to continue to vary with height.

SFL5 contains BWR assemblies with water channels to simulate reactor irradiation on three assemblies with average fuel enrichments of 2, 2.5, and 3 percent; the enrichment in each pin varies, however. The assemblies were simulated both with control blades fully inserted, and without control blades, to estimate the changes caused by these boundary conditions. The 96 fuel pins were split into 25 axial zones, with enrichment and H_2O density/void fraction varying with height. Gadolinium was also included in some of the fuel with radial zones increasing from one for just solely fuel to ten for axial zones that include Gd. Newer versions of MCNP and the associated linkage code *Monteburns* along with improved computing power allowed up to thousands of individually modeled materials to be burned instead of the ~50 material limit of the past. However, memory and processing constraints still limited the simulations to 2182 materials (2184 with blades inserted) in an infinitely-reflected BWR assembly.

In the simulations the fuel was irradiated a burnup of 48 GWd/tU in steps of 12, with 30 day cooling periods and slow start ups to account for xenon buildup. Using MCNP with CINDER90 and *Monteburns* allowed for the spent fuel libraries to be generated as a series of MCNP input files, which specify the material composition for each period in time. Cooling times of 1, 5, 20, 40, and 80 years for the assemblies were calculated with CINDER90 to determine the fuel composition after it has been removed from the reactor and stored in a spent fuel pool or dry storage. After the irradiation calculations, the Gd pins were smeared within the assemblies to reduce the number of materials represented. Additionally, the core was broken into pieces representing 1-5 different axial segments to reduce the number of materials present in each input file for DDA simulations. The resulting assemblies were then surrounded by the modified DDA instrument (see section "Results") and neutron generator; subsequent neutron transport to the detectors was then simulated with MCNP.

Table 1. Cases in SFL5

Average IE/BU	Low	Medium	High
12 GWd/MTU	X X	X X	X X
24 GWd/MTU	X X	X X	X X
36 GWd/MTU	X X	X X	X X
48 GWd/MTU	X X	X X	X X

X = Without Control Blade During Irradiation
X = With Control Blade During Irradiation

Results

The Differential Die Away instrument uses short neutron pulses generated by an external neutron generator to actively interrogate the material within a spent fuel assembly. The measured response is then predominantly prompt neutrons from induced fission of ^{235}U, ^{239}Pu, and ^{241}Pu detected by ^{3}He tubes positioned around the assayed SFA. Due to its rich and complex dynamic response with different information able to be obtained from different time windows of measurement, the neutron-generator-driven DDA technique is considered a potential candidate for high-accuracy applications (e.g., in nuclear fuel reprocessing plants or geologic repositories) [4].

The primary purpose of this study is to demonstrate that the simulated results of NDA of BWR assemblies with nearly identical DDA design exhibits similar features as the simulated results for PWR assemblies. Therefore analytical approaches developed for the PWR assemblies could be adopted or easily modified for the BWR assemblies. In the subsequent chapters we will compare the unavoidable differences in the design of the DDA instrument for assay of PWR and BWR assemblies, explain how multiplication as well as ^{235}U and Pu content varies along the longitudinal SFA axis and present comparisons of the most significant features of the instruments response and how it differs for each type of SFA's. Specifically, we'll compare contribution of burst neutrons to the overall DDA signal, the DDA signal in the so-called "magic time window" of 100-200μs with respect to varying IE, BU and CT and we'll also demonstrate how accurately can the $^{239}Pu_{eff}$ mass be restored in case of the BWR assemblies.

Design of the DDA instrument

The design of the DDA instrument that was used in the majority of the current simulations of the NDA of PWR assemblies was originally created by Pauline Blanc in 2011. It foresaw integration of the DDA technique with the delayed neutron technique (DN) [5]. For this reason, as can be seen in the left panel of **Fig. 2**, only 6 out of 8 ^{3}He detectors are encapsulated in Cd liner (2 front and 4 back detectors). One of the key features of this design is that the instrument, in the form of a collar made of Pb shielding, individual ^{3}He detectors and NG encapsulated in the tailoring material, tightly encompasses the SFA which size is ruled by the size of the 17x17 pin matrix. Since the size of the BWR assembly to be simulated is significantly smaller, defined by the 10x10 pin matrix, we faced a choice of either "shrinking" the Blanc's design in order to encompass the BWR assembly as tightly as in the case of PWR design or to keep the size of the design the same and leave a gap between the BWR SFA and the instrument itself. Since the latter option would create a new environment with possibly unexpected and not yet understood consequences we chose the earlier one. The "shrunk" DDA design as created by Kiwhan Chung in 2013 can be seen in right panel of the Fig.2.

While the number of the detectors, their geometry as well as the dimensions of the encapsulating moderator and Cd liner remained the same, the relative position of the detectors with respect to NG and SFA itself slightly changed. We, however, expect this difference to cause only an increase in the relative contribution of burst neutrons (neutrons which get detected after only a minimal re-scattering not causing any fission) primarily in the front detectors which are now positioned in much more direct line of sight with respect to the NG. The difference in the size and shape of the lead shielding, tailoring and reflecting material (tungsten and stainless steel) is not likely to change quality of the signal (i.e. how it varies with different properties of the SFA) but can be expected to influence the magnitude of the signal, i.e. how many neutrons gets reflected and/or their energies tailored, and how many will have a chance to enter the BWR SFA (due to the smaller solid angle with respect to PWR SFAs) and possibly cause fission. We therefore expect, that the difference of the quality of the signal, i.e. "the physics" of the NDA, will change primarily, if at all, due to the isotopic composition of the SFA, that is ruled by the same processes as in the case of the PWR assemblies, but in a very different environment of moderator of varying density, pressure and temperature.

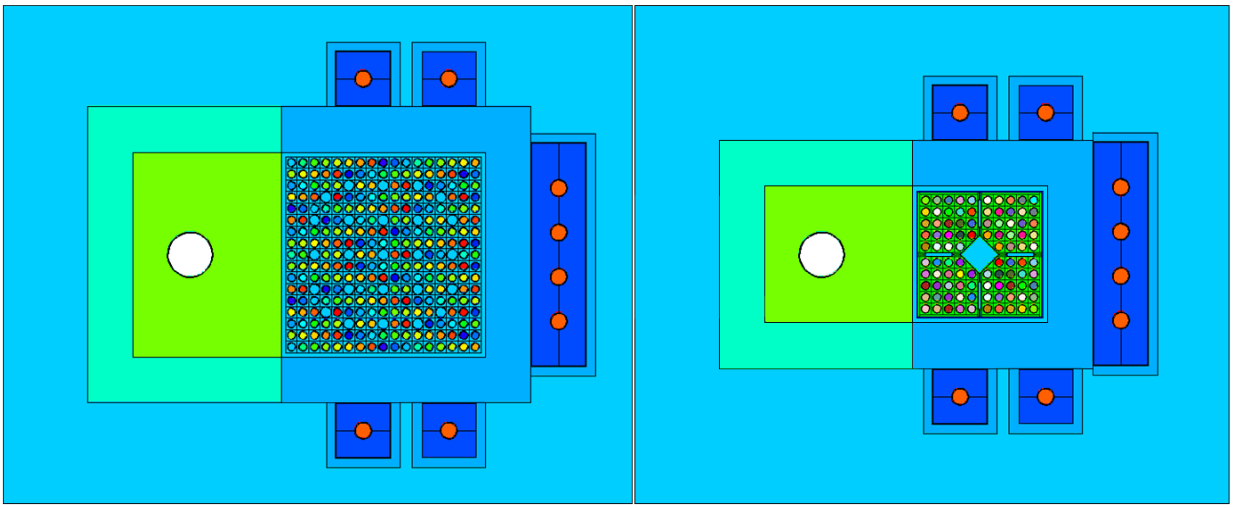

Fig. 2: *Cross sectional view of the DDA design geometry as simulated with the MCNP for the PWR (left) and BWR (right) SFAs.*

Axial profile of BWR assemblies

Axial burn-up profile of BWR SFAs is often cited as the most important additional degree of complexity when compared to the PWR SFAs. As introduced in the "methodology" section, model of any BWR SFA in SFL5 consists of 25 axial region of the same height in which the distribution of individual isotopes varies from pin to pin, but is considered homogeneous in individual pins. In order to confront computational limitations when simulating the DDA instruments response to active interrogation of the BWR at various positions along its longitudinal axis, we "positioned" the DDA instrument at the center height of the axial region of interest but also included two axial region above and two below the region to which the DDA instrument was attached. Thus, for example, when simulating the DDA response at the position of the 13^{th} axial region, the simulation would include also regions 11, 12, 14 and 15. Axial regions 1-10 and 16-25 would not be part of the simulation, and their contribution to the overall DDA signal with detector at the position of the 13^{th} axial region is, for the purpose of this study, not quantified, and in general considered negligible.

The **Fig.3** displays the axial burn-up profile in terms of various isotopic contents or physical quantities per axial segment for three different BWR SFAs, with the numbering of the segments being

proportional to the height of the SFA (i.e. seg #1 is the lowest part of the SFA at the bottom of the reactor vessel, and seg.# 25 being the highest segment of the SFA). However, due to the edge effects not yet properly simulated at the time of this study only segments 4-22 were analyzed and are thus displayed in Fig.3.

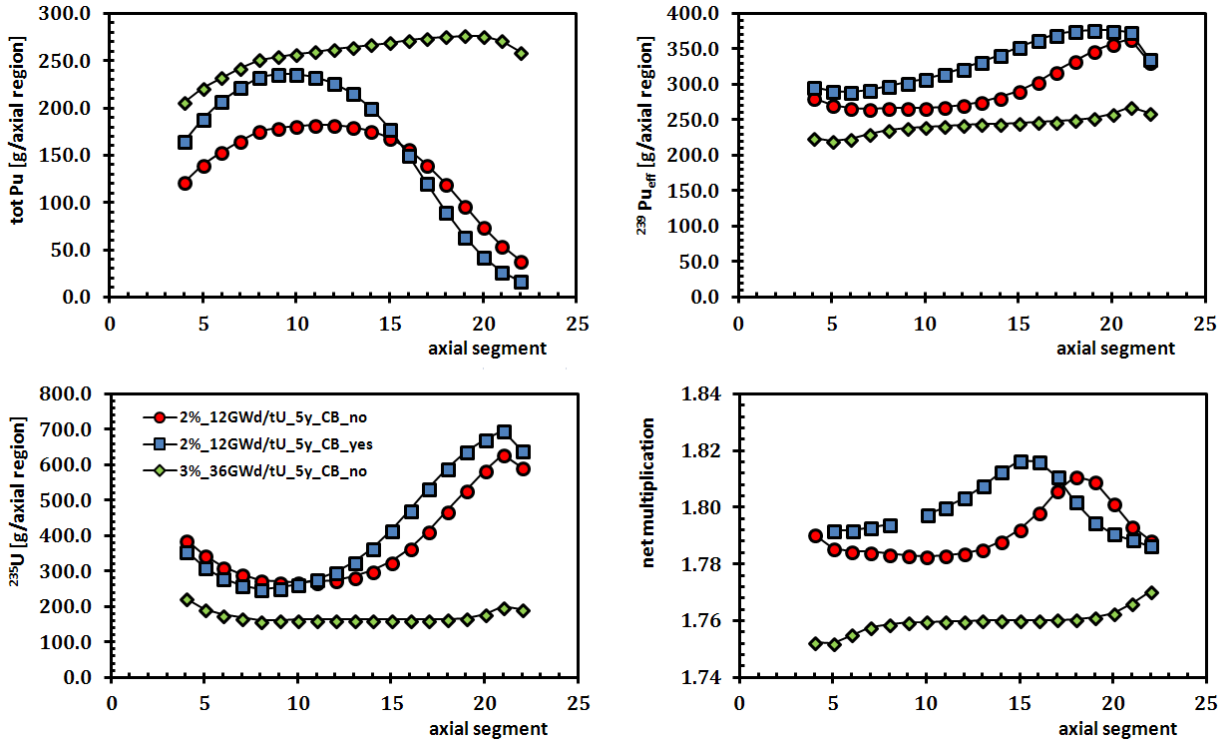

Fig. 3: *Axial profile of selected characteristics for three different BWR SFA's*

While we are not yet capable of simulating the detailed axial profile for each of the SFAs of SFL5, the example profiles of selected quantities in Fig.3 for the three chosen SFAs demonstrate well how complex the evolution of each SFA characteristic along the longitudinal axis may be with changing IE, BU, CT and inclusion or the lack off of the control blades. As indicated in the lower left panel of Fig. 3, the ^{235}U is first burned in the lower part of SFA, and only with higher overall BU the burn-up along the longitudinal axis becomes more uniform. The ^{235}U isotopic content decreases as Pu isotopes build in, be it ^{239}Pu, ^{240}Pu or in the case displayed in the Fig.3 the sum of all Pu isotopes. As a consequence, the burning of ^{235}U is to a certain level compensated by the breeding of Pu, therefore the variation of ^{239}Pu$_{eff}$ along the longitudinal axis that reflects the total fissile content according to

$$m[^{239}\mathrm{Pu}_{eff}] = 0.5 \times m[^{235}\mathrm{U}] + m[^{239}\mathrm{Pu}] + 1.33 \times m[^{241}\mathrm{Pu}], \quad (1)$$

does not vary nearly as much as the content of the individual fissile isotopes. However, since initial burnup of the fuel rod occurs at the bottom of the reactor where there is more moderator (i.e. water) than at the top where there is steam, the preferential burning of ^{235}U at the bottom of the reactor for low BU SFAs results in greater concentration of neutron absorbers (fission products and minor actinides) the local multiplication does not copy the trend of ^{239}Pu$_{eff}$ and exhibits a peak in the upper half of the SFA because more ^{235}U is present and fewer neutron absorbers. Nevertheless, with ever increasing overall burnup, the maximum of multiplication seems to smooth out, resulting in a rather monotonous trend as seen in the lower right panel of Fig.3 for the fully burned SFA with the average IE of 3% and BU of 36 GWd/tU.

The results displayed in Fig.3 thus implies that should we be able to determine the axial profile of various quantities, we may be able to determine certain SFA parameters, such as BU, just from its shape. But in order to gain the possible capability to determine BU (or other characteristic) of the SFA the detailed evolution of the shape of axial profiles would need to be simulated and analyzed for the substantial (if not the entire) SFL5. Such task would require an enormous effort that currently exceeds our computational as well as human resources.

On the other hand, being aware of the great differences in isotopic composition along the longitudinal axis of the SFA and its likely implication on the DDA instruments response, we simulated active interrogation of the majority of SFA's from SFL5 for three axial regions – 5, 13, and 21 – each being thus representative of the entire lower, central and upper region of the SFA. Considering the selection of average IE of 2.0, 2.5 and 3.0%, average BU of 12, 24, 36, and 48 GWd/tU, CT of 5, 20, and 50 y, presence or absence of control blades, and the three selected axial regions, 216 simulations were performed to map the DDA instruments response as function of these global BWR SFA characteristics.

Contribution of burst neutrons to the total active DDA signal

The signal, i.e. neutrons, that the DDA instrument measures can be divided into its passive and active part. The passive part is primarily made of neutrons that come from processes initiated by the spontaneous fission inside the SFA. The active part of the signal is a consequence of the active interrogation that is in the case of this instrument realized by the injection of neutrons into the SFA by an external neutron generator. But not all neutrons cause fission in the SFA. Significant part of the neutrons from the neutron generator can rescatter in and around the SFA and can enter the ^{3}He detectors without causing any fission at all. These neutrons, although being part of the active signal, thus do not carry any information on the fissile content of the SFA and essentially create an undesired background with respect to the neutrons that do cause fission (i.e. "fission neutrons"), carry information about the SFAs composition, and are essentially the desired signal to be measured.

The ability to properly account for the contribution of the burst neutrons with respect to the fission neutrons is an imperative in order to properly evaluate the DDA signal. In case of the PWR assemblies, it was found that while the relative contribution of burst neutrons varies significantly among the SFAs, the absolute contribution is nearly constant, meaning that burst neutrons create a constant background which once determined for one SFA can be used to correct the active signal for any other SFA as well [4].

For the purpose of this study, we evaluated the absolute probability of detecting a burst neutron per source neutron from NG and the relative contribution to the total active DDA signal in the time window of 100-200μs. The results are displayed in **Fig.4** for 216 BWR SFA, while the **Table 2** lists the general SFA characteristics associated with each SFA number.

The results in the left panel of Fig.4 indicate that as in the PWR SFAs, also in case of BWR SFAs the absolute number of burst neutrons per source neutron from the NG varies only slightly (8.57e-5 +/- 0.3%) and can be for any practical purposes considered constant. However, the results in the right panel suggest that the relative contribution of burst neutrons to the total active signal varies greatly between 25 and 60%, implying that in many instances the DDA instrument measures more burst neutrons than fission neutrons in the prominent time window of 100-200μs. This is in contrast to the PWR results where, in case of SFL1 and the identical time window, the relative contribution of the burst neutrons varied only between 5 and 28%.

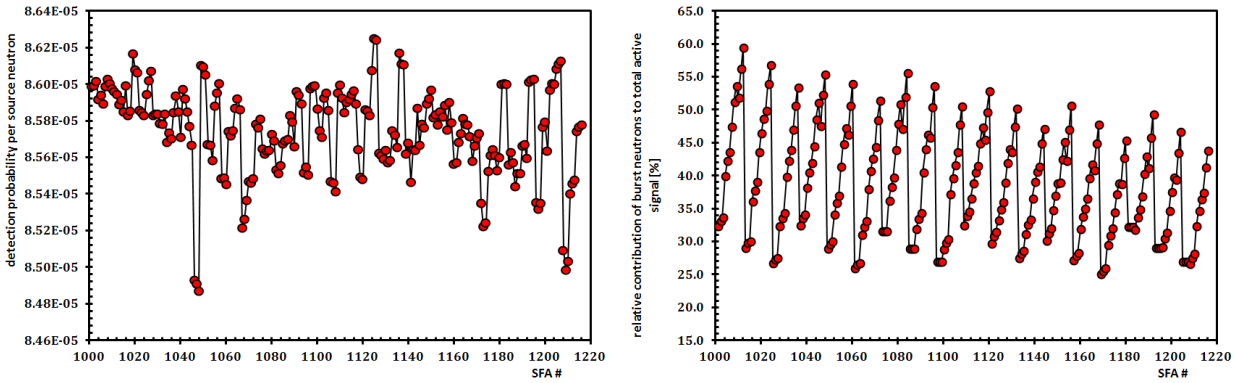

Fig. 4: *Absolute detection probability of a burst neutron per source neutron from the NG (left) and the relative contribution of burst neutrons to the total active signal as function of the SFA number (see Table 2 for parameters of individual SFAs)*

Since it is not yet resolved how the absolute number of burst neutrons in the total active signal will be determined, it is not possible to exactly evaluate the impact of subtracting relatively large background of yet unknown uncertainty from the active signal. On the other, the unfavorable comparison of burst neutron results for BWR SFAs with respect to PWR SFAs should initiate design changes that could help minimize the burst neutron contribution. Among the most detrimental changes should be the position of the front detectors and/or the NG, so these two instrument components do not lie in the direct line of sight of each other. Alternatively, an additional shielding of front detectors from the burst neutrons may need to be incorporated. Also, considering the different mechanisms that rule the die-away time of the burst neutron population and the fission neutron population, the thickness of the poly moderator around the ^{3}He detectors may need to be reduced. That way the population of burst neutrons would die-away faster than the fission neutrons whose population die-away time is ruled by the SFA composition. Additionally, as suggested previously [6] the choice of interrogation scenario does influence the relative contribution of the burst neutrons and therefore may be consciously modified to improve fission-to-burst neutron ratio.

Magic time window and measurement of the multiplication

Multiplication is one of the main characteristics of any SFA. It primarily depends on the composition and geometry of the spent fuel and is thus an implicit function of the irradiation history and parameters of the SFA, such as IE, BU and CT. The process of multiplication of the external neutron flux inside the SFA is the key process that allows us to perform the NDA with the DDA instrument. In case of the previous analysis of simulations of the PWR assemblies, the multiplication played a key role in establishing the so-called "magic time window" in which IE and BU of SFA can be determined [7] and in which die-away time can be used to correct the DDA signal in order to reconstruct the total fissile content in terms of $^{239}Pu_{eff}$ [8]. We have also shown that multiplication in conjunction with passive neutron measurement can be explicitly used to determine the total Pu content [9].

It is thus essential to demonstrate that even for the BWR SFAs with a complex shape of the axial burnup profile the multiplication (at least in the "local sense") can be determined without a prior knowledge of the irradiation history parameters. In case of the PWR assemblies, we showed that multiplication can be determined by four different methods (total integrated DDA signal, DDA signal in 100-200μs time domain, front-to-back detector ratio and die-away time in 500-1000μs time domain) [4]. For the purpose of this study, we'll concentrate only on the method utilizing the DDA signal in a discrete time domain. The **Fig. 5** displays the net DDA signal (fission neutrons only) as function of net multiplication in five different time domains: 0-50μs, 50-100μs, 100-200μs, 200-500μs and 500-1000μs for 108 BWR SFAs without control blades (left column) and 108 BWR SFAs with control blades (right

column) for which the IE varies between 2.0, 2.5 and 3.0%, BU varies between 12, 24, 36, and 48 GWd/tU, CT varies between 5, 20, and 50y and the DDA signal is simulated at three different vertical positions – 5, 13 and 21. Due to the great dynamic range, the individual points in the figure are not distinguished according to the SFA parameters, however the degree of alignment or presence of structure illustrates the universal correlation of the given DDA signal with respect to multiplication.

Table 2: *Parameters of individual SFAs associated with the SFA number*

SFA #	IE [%]	BU [GWd/tU]	CT [y]	Contr. blades	axial seg	SFA #	IE [%]	BU [GWd/tU]	CT [y]	Contr. blades	axial seg	SFA #	IE [%]	BU [GWd/tU]	CT [y]	Contr. blades	axial seg
1001	2.0	12	5	n	5	**1037**	2.0	12	5	n	13	**1073**	2.0	12	5	n	21
1002	2.0	12	20	n	5	**1038**	2.0	12	20	n	13	**1074**	2.0	12	20	n	21
1003	2.0	12	50	n	5	**1039**	2.0	12	50	n	13	**1075**	2.0	12	50	n	21
1004	2.0	24	5	n	5	**1040**	2.0	24	5	n	13	**1076**	2.0	24	5	n	21
1005	2.0	24	20	n	5	**1041**	2.0	24	20	n	13	**1077**	2.0	24	20	n	21
1006	2.0	24	50	n	5	**1042**	2.0	24	50	n	13	**1078**	2.0	24	50	n	21
1007	2.0	36	5	n	5	**1043**	2.0	36	5	n	13	**1079**	2.0	36	5	n	21
1008	2.0	36	20	n	5	**1044**	2.0	36	20	n	13	**1080**	2.0	36	20	n	21
1009	2.0	36	50	n	5	**1045**	2.0	36	50	n	13	**1081**	2.0	36	50	n	21
1010	2.0	48	5	n	5	**1046**	2.0	48	5	n	13	**1082**	2.0	48	5	n	21
1011	2.0	48	20	n	5	**1047**	2.0	48	20	n	13	**1083**	2.0	48	20	n	21
1012	2.0	48	50	n	5	**1048**	2.0	48	50	n	13	**1084**	2.0	48	50	n	21
1013	2.5	12	5	n	5	**1049**	2.5	12	5	n	13	**1085**	2.5	12	5	n	21
1014	2.5	12	20	n	5	**1050**	2.5	12	20	n	13	**1086**	2.5	12	20	n	21
1015	2.5	12	50	n	5	**1051**	2.5	12	50	n	13	**1087**	2.5	12	50	n	21
1016	2.5	24	5	n	5	**1052**	2.5	24	5	n	13	**1088**	2.5	24	5	n	21
1017	2.5	24	20	n	5	**1053**	2.5	24	20	n	13	**1089**	2.5	24	20	n	21
1018	2.5	24	50	n	5	**1054**	2.5	24	50	n	13	**1090**	2.5	24	50	n	21
1019	2.5	36	5	n	5	**1055**	2.5	36	5	n	13	**1091**	2.5	36	5	n	21
1020	2.5	36	20	n	5	**1056**	2.5	36	20	n	13	**1092**	2.5	36	20	n	21
1021	2.5	36	50	n	5	**1057**	2.5	36	50	n	13	**1093**	2.5	36	50	n	21
1022	2.5	48	5	n	5	**1058**	2.5	48	5	n	13	**1094**	2.5	48	5	n	21
1023	2.5	48	20	n	5	**1059**	2.5	48	20	n	13	**1095**	2.5	48	20	n	21
1024	2.5	48	50	n	5	**1060**	2.5	48	50	n	13	**1096**	2.5	48	50	n	21
1025	3.0	12	5	n	5	**1061**	3.0	12	5	n	13	**1097**	3.0	12	5	n	21
1026	3.0	12	20	n	5	**1062**	3.0	12	20	n	13	**1098**	3.0	12	20	n	21
1027	3.0	12	50	n	5	**1063**	3.0	12	50	n	13	**1099**	3.0	12	50	n	21
1028	3.0	24	5	n	5	**1064**	3.0	24	5	n	13	**1100**	3.0	24	5	n	21
1029	3.0	24	20	n	5	**1065**	3.0	24	20	n	13	**1101**	3.0	24	20	n	21
1030	3.0	24	50	n	5	**1066**	3.0	24	50	n	13	**1102**	3.0	24	50	n	21
1031	3.0	36	5	n	5	**1067**	3.0	36	5	n	13	**1103**	3.0	36	5	n	21
1032	3.0	36	20	n	5	**1068**	3.0	36	20	n	13	**1104**	3.0	36	20	n	21
1033	3.0	36	50	n	5	**1069**	3.0	36	50	n	13	**1105**	3.0	36	50	n	21
1034	3.0	48	5	n	5	**1070**	3.0	48	5	n	13	**1106**	3.0	48	5	n	21
1035	3.0	48	20	n	5	**1071**	3.0	48	20	n	13	**1107**	3.0	48	20	n	21
1036	3.0	48	50	n	5	**1072**	3.0	48	50	n	13	**1108**	3.0	48	50	n	21
1109	2.0	12	5	y	5	**1145**	2.0	12	5	y	13	**1181**	2.0	12	5	y	21
1110	2.0	12	20	y	5	**1146**	2.0	12	20	y	13	**1182**	2.0	12	20	y	21
1111	2.0	12	50	y	5	**1147**	2.0	12	50	y	13	**1183**	2.0	12	50	y	21
1112	2.0	24	5	y	5	**1148**	2.0	24	5	y	13	**1184**	2.0	24	5	y	21
1113	2.0	24	20	y	5	**1149**	2.0	24	20	y	13	**1185**	2.0	24	20	y	21
1114	2.0	24	50	y	5	**1150**	2.0	24	50	y	13	**1186**	2.0	24	50	y	21
1115	2.0	36	5	y	5	**1151**	2.0	36	5	y	13	**1187**	2.0	36	5	y	21
1116	2.0	36	20	y	5	**1152**	2.0	36	20	y	13	**1188**	2.0	36	20	y	21
1117	2.0	36	50	y	5	**1153**	2.0	36	50	y	13	**1189**	2.0	36	50	y	21
1118	2.0	48	5	y	5	**1154**	2.0	48	5	y	13	**1190**	2.0	48	5	y	21
1119	2.0	48	20	y	5	**1155**	2.0	48	20	y	13	**1191**	2.0	48	20	y	21
1120	2.0	48	50	y	5	**1156**	2.0	48	50	y	13	**1192**	2.0	48	50	y	21
1121	2.5	12	5	y	5	**1157**	2.5	12	5	y	13	**1193**	2.5	12	5	y	21
1122	2.5	12	20	y	5	**1158**	2.5	12	20	y	13	**1194**	2.5	12	20	y	21
1123	2.5	12	50	y	5	**1159**	2.5	12	50	y	13	**1195**	2.5	12	50	y	21
1124	2.5	24	5	y	5	**1160**	2.5	24	5	y	13	**1196**	2.5	24	5	y	21
1125	2.5	24	20	y	5	**1161**	2.5	24	20	y	13	**1197**	2.5	24	20	y	21
1126	2.5	24	50	y	5	**1162**	2.5	24	50	y	13	**1198**	2.5	24	50	y	21
1127	2.5	36	5	y	5	**1163**	2.5	36	5	y	13	**1199**	2.5	36	5	y	21
1128	2.5	36	20	y	5	**1164**	2.5	36	20	y	13	**1200**	2.5	36	20	y	21
1129	2.5	36	50	y	5	**1165**	2.5	36	50	y	13	**1201**	2.5	36	50	y	21
1130	2.5	48	5	y	5	**1166**	2.5	48	5	y	13	**1202**	2.5	48	5	y	21
1131	2.5	48	20	y	5	**1167**	2.5	48	20	y	13	**1203**	2.5	48	20	y	21
1132	2.5	48	50	y	5	**1168**	2.5	48	50	y	13	**1204**	2.5	48	50	y	21
1133	3.0	12	5	y	5	**1169**	3.0	12	5	y	13	**1205**	3.0	12	5	y	21
1134	3.0	12	20	y	5	**1170**	3.0	12	20	y	13	**1206**	3.0	12	20	y	21
1135	3.0	12	50	y	5	**1171**	3.0	12	50	y	13	**1207**	3.0	12	50	y	21
1136	3.0	24	5	y	5	**1172**	3.0	24	5	y	13	**1208**	3.0	24	5	y	21
1137	3.0	24	20	y	5	**1173**	3.0	24	20	y	13	**1209**	3.0	24	20	y	21
1138	3.0	24	50	y	5	**1174**	3.0	24	50	y	13	**1210**	3.0	24	50	y	21
1139	3.0	36	5	y	5	**1175**	3.0	36	5	y	13	**1211**	3.0	36	5	y	21
1140	3.0	36	20	y	5	**1176**	3.0	36	20	y	13	**1212**	3.0	36	20	y	21
1141	3.0	36	50	y	5	**1177**	3.0	36	50	y	13	**1213**	3.0	36	50	y	21
1142	3.0	48	5	y	5	**1178**	3.0	48	5	y	13	**1214**	3.0	48	5	y	21
1143	3.0	48	20	y	5	**1179**	3.0	48	20	y	13	**1215**	3.0	48	20	y	21
1144	3.0	48	50	y	5	**1180**	3.0	48	50	y	13	**1216**	3.0	48	50	y	21

Since in the very early (0-50μs) and very late (500-1000μs) time domains the data points are clearly scattered along some general trend, these time domains cannot be used for precise determination of the multiplication from the DDA signal alone. On the other hand, no matter what are the exact SFA parameters, in the time domains of 100-200μs for SFAs without the control blades and 50-100μs for SFAs with control blades the DDA signal scales the best and, in fact, nearly perfectly with the multiplication. In analogy to PWR results, these two time domains for their respective classes of SFAs can be called "magic time window".

While it is obvious that a more detailed analysis could help to narrow and more accurately determine the precise range of the time interval in which DDA signal is an exact measure of the multiplication, the results seem to indicate that such "magic time window" is indeed different depending on the presence or absence of the control blades. The reason for such effect of control blades is currently not understood.

On the other hand, despite great variation of axial burnup profile with respect to various SFA parameters, the magic time window seems to be the same, no matter of the differences in the magnitude of the DDA signal with changing position along the SFA longitudinal axis.

In conclusion of this subsection, even for BWR SFAs we have demonstrated that the magic time window can be established independent of the axial segment assayed and therefore also the multiplication of the associated part of the SFA can be determined a directly compared between axial regions of the same SFA.

(Note: the 6 groups of points that significantly deviate from the linear trend in plots for 50-100μs time domains belong to SFA's with BU of 12 GWd/tU at axial region 21. It is not clear why these results deviate so much from the universal trend but an error in simulations is suspected and the results for these SFAs will be excluded from any further analyses)

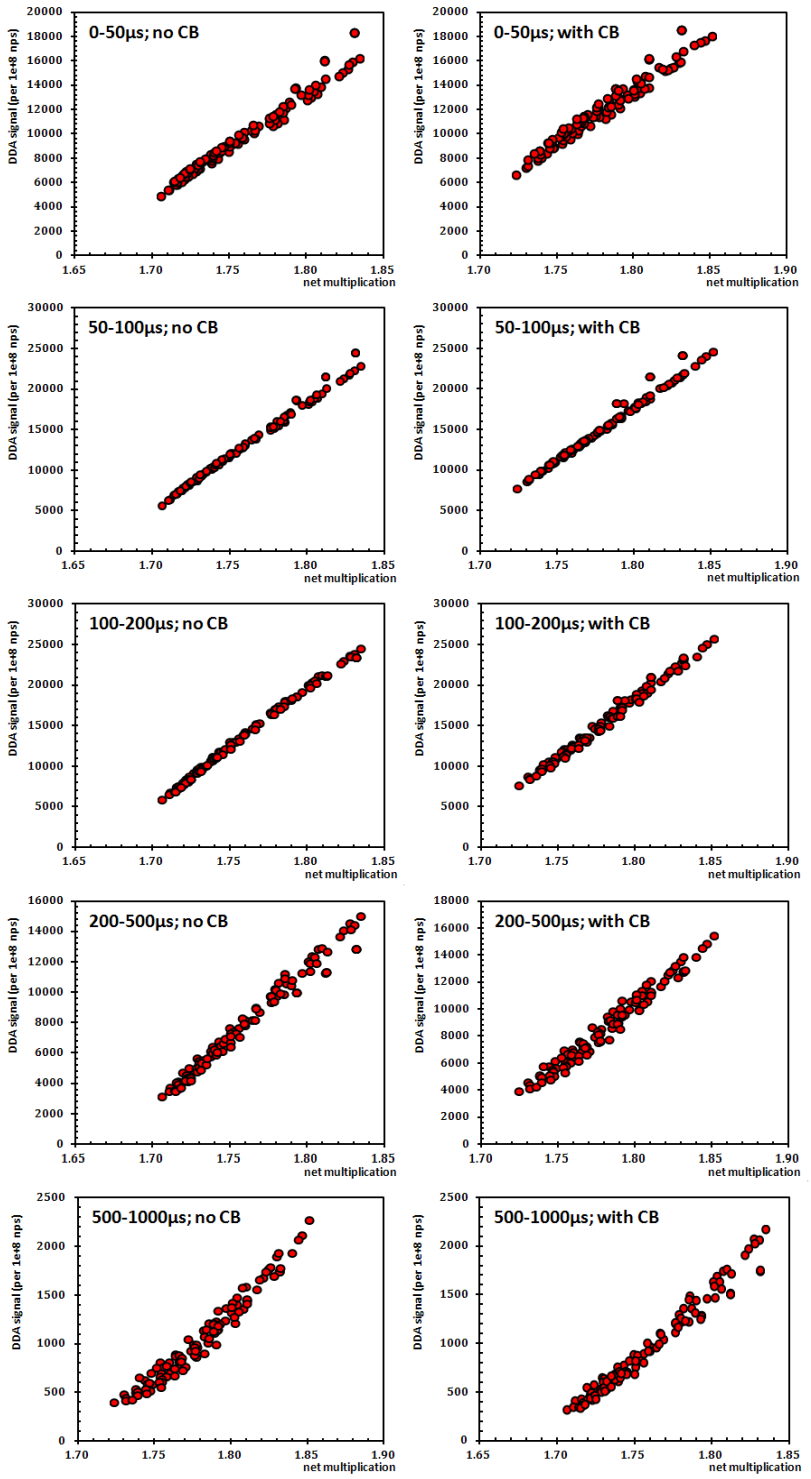

Fig. 5*: DDA signal as the function of the net multiplication of the BWR SFA in various time domains for SFA with (left) and without (right) control blades.*

Determination of IE and BU of BWR SFAs with the DDA instrument

One of the most prominent and promising results of the analysis of the DDA instruments response to active interrogation of PWR assemblies has been the finding that the die-away time of the net active DDA signal (i.e. fission neutrons only) in the so called "magic time window" of 100-200μs can allow for determination of the IE and BU of the SFA, as demonstrated in the **Fig.6** (reprinted from [7]). Unfortunately, the results of simulations of the BWR SFAs do not yield such clear discriminatory features, as can be seen with respect to average IE in left panel of **Fig.7** and with the respect to the average BU in the right panel of Fig.7.

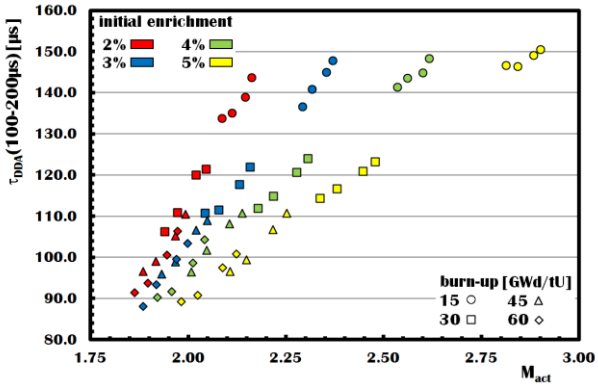

Fig.6: *Die-away time constant (τ_{DDA}) as a function of active multiplication M_{act} for 64 SFA's from SFL-1 (left) as determined for the DDA signal measured in the time windows of 100-200 μs (reprinted from [4]).*

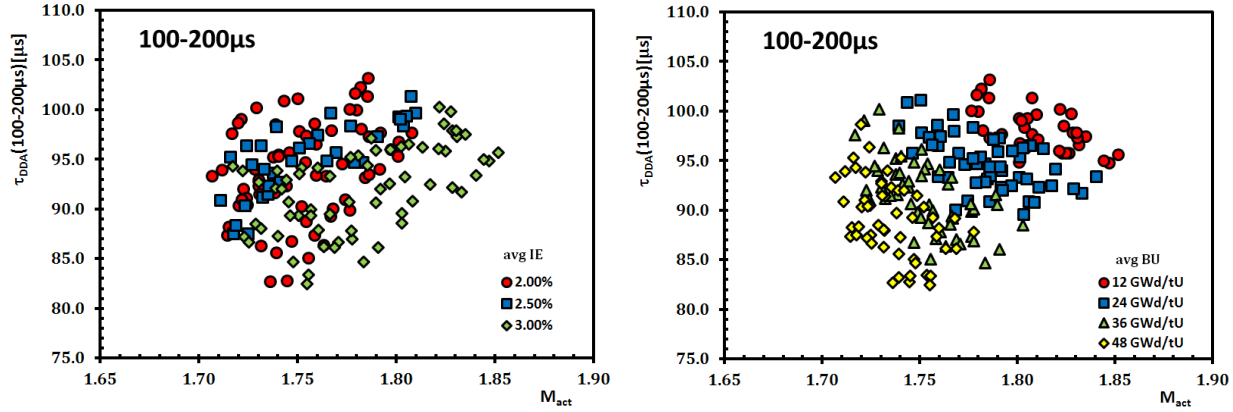

Fig.7: *Die-away time constant (τ_{DDA}) as a function of active multiplication M_{act} for 216 SFA's from SFL-5 as determined for the DDA signal measured in the time windows of 100-200 μs with respect to the SFA average IE (left) and BU (right).*

While both panels of Fig.7 seem rather unfavorable in terms of determining IE or BU compared to Fig.6, it should be noted that data in Fig.6 related to SFL-1 are much more "homogenous" in nature than data in Fig.7. In case of SFL1, all SFA's are "burned" in a very similar manner, creating thus a straight forward relation between resident fissile material and neutron absorbers. In case of SFL5, each segment of SFA is burned differently due to the different properties of the surrounding moderator (i.e. water vs. vapor). This results in a different relation between the resident fissile mass and the neutron absorbers which affect most significantly the die-away of the DDA signal, leading to intermixing of data corresponding to different IE, and BU. Such effect was first observed when die-away time in 100-200μs time domain was compared for SFL1 and SFL2a although on a much smaller scale. When comparing

these two libraries the difference between them is primarily in the concentration of neutron absorbers (due to different simulation of burning) while the fissile content is nearly the same. The **Fig.8** illustrates how results of SFL1 and SFL2a overlap with each other in the region of high BU, even though they are clearly discriminatory with respect to IE and BU within an individual SFL data set.

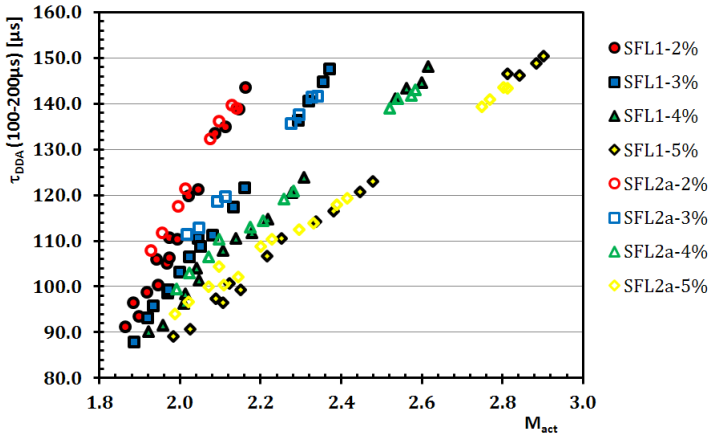

Fig.8: *Comparison of die-away time constants from SFL1 and SFL2a as a function of active multiplication M_{act} as determined for the DDA signal measured in the time windows of 100-200µs*

Therefore, in order to reconstruct the discriminatory properties of the die-away time constants with respect to IE and BU, it is necessary to divide the SFL5 data into sets which were "burned" under similar conditions, i.e. by the axial segment and the presence or absence of the control blades. This, in case of the SFL5, means a division into 6 different groups, each with 36 SFAs varying in IE, BU and CT only (*Note: data for SFAs with BU of 12GWd/tU at seg 21 were excluded from the analyses*). **Fig.9** displays the die-away times in 100-200µs time domain as function of the net multiplication in each of the SFL5 subsets.

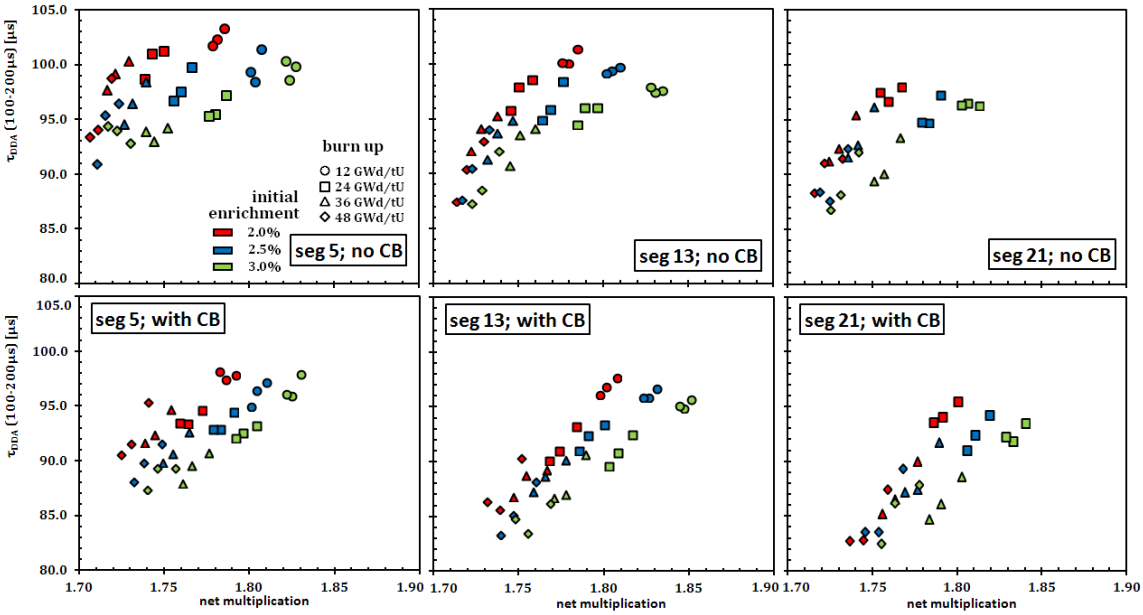

Fig.9: *Comparison of die-away time constants for six groups of SFAs from SFL5 (differing in presence or absence of control blades and the vertical position of the DDA instrument)as a function of the net multiplication as determined for the DDA signal measured in the time windows of 100-200 µs.*

As can be seen from the results in individual panels of Fig.9, the discriminatory nature of the die-away time has been restored, although it does not reach the same quality as the results for PWR assemblies in Fig.6. In order to understand the qualitative difference between the results for PWR and BWR assemblies it needs to be realized that due to the smaller size of the BWR assemblies the dynamic range of the multiplication is significantly smaller than in case of the PWR assemblies. While in the case of PWR assemblies in SFL-1 the multiplication varies from 1.86 to 2.90 (or 2.37 should we limit ourselves to SFAs with IE only between 2 and 3%), in case of BWR assemblies from SFL5 it varies only between 1.71 and 1.85. The multiplication then defines the die-away time whether implicitly in time domain of 100-200μs or explicitly in time domain of 500-1000μs [4]. This translates in case of the 100-200μs in reduction of dynamic range of die-away times from 88-152μs (or 148μs for SFA with IE≤3%) in case of SFL1 to 83-103μs range in case of SFL5. Furthermore, for individual groups of SFAs as in Fig.9 the dynamic range of the die-away times is typically even smaller, only around 10-15μs long.

Therefore, when considering the typical error of determining the die-away time from the exponential fit of the DDA signal in a given time domain being ~2-3μs, the overlapping results for different IE and BU come as no surprise. However, it also should be considered, as currently believed, it is predominantly the statistical uncertainty that defines the error of the die-away times and that is ruled by the number of neutron histories simulated by the MCNP. In the simulations used in this study in case of each SFA the total of $5x10^8$ neutrons emerging from the neutron generator were simulated. While this represents maximum reasonably achievable statistics in the simulations, it also represents only about 5s of a real life measurement should the intensity of the neutron generator be $1x10^8$ n/s. We can then expect that with the real-life measurement being on the order of several minutes, the statistical errors should be significantly diminished and precision of determination of die-away time should be greatly improved. It can, of course, be argued, that systematic errors due to the measurement itself may prevent more precise determination of the die-away times. However, considering the currently foreseeable systematic errors such as subtraction of the passive background, SFA positioning error, NG strength calibration and monitoring and detector thermal stability, we may expect the differential information such as die-away time remain largely unaltered, even though such systematic errors could influence the overall magnitude of the signal.

Thus despite being unable to demonstrate DDA instruments ability to measure IE and BU of the BWR assemblies (at least in a qualitatively comparable way to PWR cases) through the simulation, it is considered reasonable to expect that due to greatly improved statistics the capability of the instrument will be restored in the real life measurements.

Determination of the total fissile content in the BWR SFA

Defined as the weighted sum of the major fissile isotopes in eq.(1) the correct reconstruction of the total fissile content of the SFA is currently considered as the most reliable and complex test of the DDA instruments performance. The DDA signal, in general, is driven by the competition between the fissile material and the neutron absorbers in the SFA. Thus its dependence on the fissile content itself is very complex, reflecting the amount of neutron absorbers. This, in turn, is dictated by the overall SFA parameters, such as IE, BU and CT, but also by the details of the irradiation history, and physical and chemical properties of the moderator in the reactor (as learnt from SFL3 [8]). However, since the die-away time of the DDA signal in the magic time window can be associated with the effective amount of neutron absorbers [8], it can be used for a correction of the DDA signal which becomes a smooth function of the fissile content alone. The simple correction is then of the form

$$corDDA_{100\text{-}200} = DDA_{100\text{-}200} \cdot \tau_{100\text{-}200}^{\varepsilon} \qquad (2)$$

where $corDDA_{100\text{-}200}$ is the corrected DDA signal in the time domain of 100-200μs, $DDA_{100\text{-}200}$ is the measured (i.e. uncorrected) DDA signal in the same time domain, and ε is the fitting parameter. The left panel of Fig. 10 displays the relation between the uncorrected DDA signal and the $^{239}Pu_{eff}$ in case of the SFL1 (i.e. PWR assemblies), while the right panel of Fig.10 display the same relation after the correction of the DDA signal according to eq.(2).

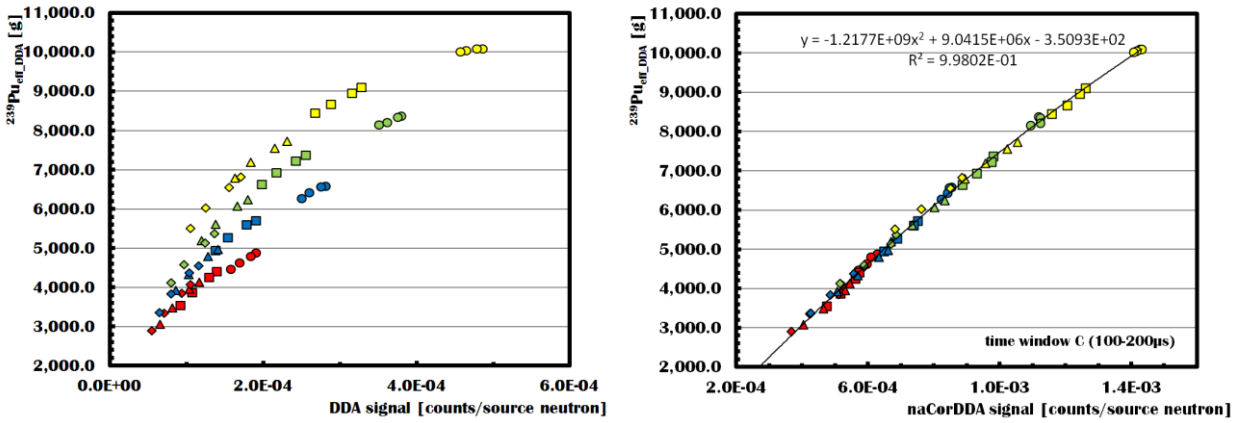

***Fig. 10**: Relationship between uncorrected and corrected DDA signal and the $^{239}Pu_{eff}$ in SFL-1.*

The **Fig. 11** then displays the error of the reconstruction of $^{239}Pu_{eff}$ from four different SFLs but all based on the same correlation from the right panel of Fig.10. In other words, one type of SFL can be used for calibration (i.e. finding the correct value of fitting parameter ε from eq.(2)) that works with other SFLs no matter what burning conditions prevailed in the reactor.

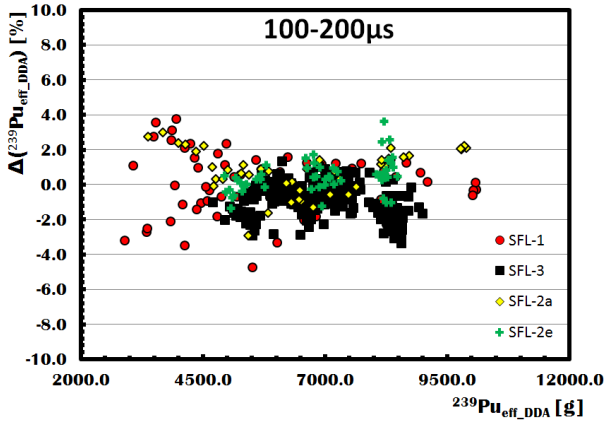

Fig.11: *Relative error of reconstructed $^{239}Pu_{eff}$ based on eq.(2) for 4 different SFLs.*

Similar approach to reconstruction of $^{239}Pu_{eff}$ can be used with simulated DDA signal in case of BWR assemblies from SFL5. However, since the amount of fissile material as well as the DDA signal varies significantly with the position of the DDA instrument along the SFA longitudinal axis, It is not possible to use correlation of the DDA signal with the total fissile content of the SFA, but rather only with the fissile material content of the part of the SFA that is being actively interrogated. For the purpose of this study, we choose fissile content in the five axial segments nearest to the DDA instrument as the relevant fissile mass to which the DDA signal is compared. This choice is to a certain degree arbitrary and a more detailed study may be needed to determine the exact size of the SFA part of which a single active

interrogation is representative of. The left panel of **Fig. 12** then displays the fissile content as defined above as function of the measured DDA signal for 198 SFAs from SFL5 (*Note: 18 SFAs with BU=12GWd/tU were excluded for suspected error in simulations*). The right panel of the same figure then displays the DDA signal corrected according to eq. (2) with value of ε being -2.03.

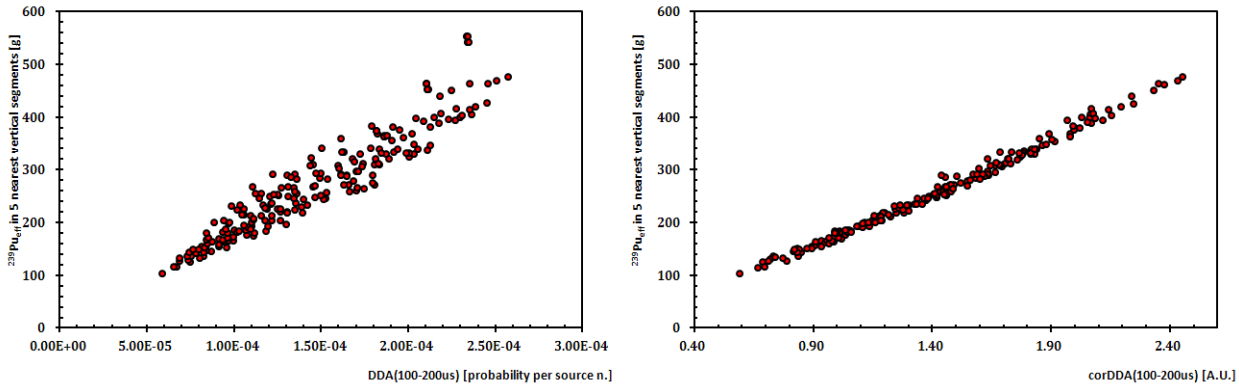

Fig.12: *Relationship between uncorrected and corrected DDA signal and the $^{239}Pu_{eff}$ in SFL-5.*

The **Fig.13** displays the error of the reconstruction of $^{239}Pu_{eff}$ in SFL5 based on the correlation in the right panel of Fig.12. While the average variation of the error in reconstructing $^{239}Pu_{eff}$ is 1.7% in case of the SFL1, it is 2.8% in case of the BWR assemblies from SFL5. Such increase is not negligible, but is likely to be reduced, if not eliminated, should the precision of the die-away times used for the correction of the DDA signal be same in SFL5 as is in the SFL1. Nevertheless, the successful reconstruction of the $^{239}Pu_{eff}$ masses in SFL5, although related only to a limited part of the SFA, suggests that the underlying physical principles that were used in the analysis of the PWR simulated NDA can be used in case of the BWR NDA as well.

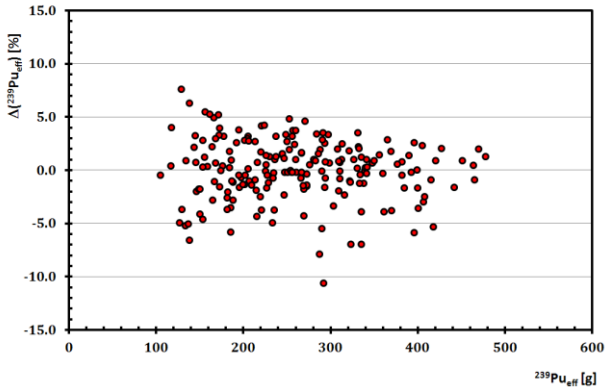

Fig.13: *Relative error of reconstructed $^{239}Pu_{eff}$ based on eq.(2) for SFL5.*

Conclusion

Overall, based on the analysis of more than 266 MCNP simulations of active interrogation of various regions of BWR SFAs from SFL5, we conclude that the DDA instrument is capable of achieving qualitatively same results as in the case of the NDA of the PWR assemblies. However, geometrical differences, such as size, and, above all, the principally different irradiation conditions in the reactor results in significant, but not prohibitive, challenges in accurate determination of the various SFA characteristics such as multiplication, IE, BU, and total fissile content. But it is believed that such

challenges can be successfully overcome through adaptation of the instrument design, proper mapping of the signal variation with respect to the longitudinal axis, and enhanced statistics easily achievable in real life measurements but unaffordable in the simulations.

Acknowledgements:

The authors would like to thank Kiwhan Chung for providing the source files with the modified DDA design with which the majority of the simulations in this study were carried out.

References:

[1] M. A. Humphrey, S. J. Tobin, and K. D. Veal, "The Next Generation Safeguards Initiative's Spent Fuel Nondestructive Assay Project," *Journal of Nuclear Materials Management* Vol. 40, No.3, pgs. 6-11 (2012).

[2] J. D. Galloway, H. R. Trellue, M. L. Fensin, and B. L. Broadhead, "Design and Description of the NGSI Spent Fuel Library with an Emphasis on Passive Gamma Signal," *Journal of Nuclear Materials Management*, Vol. **40**, No. *3*, p. 25 (2012).

[3] N. A. Fischer, H. R. Trellue, and J. D. Galloway, "Rapid Light Water Reactor modeling for MCNP and Associated Boiling Water Reactor Library," American Nuclear Society 2013 Annual Meeting Transactions, Atlanta, Georgia (June 16-20, 2013) and Los Alamos National Laboratory report LA-UR-13-24242.

[4] V. Henzl, M. T. Swinhoe, S. J. Tobin, and H. O. Menlove, "Measurement of the Multiplication of a Spent Fuel Assembly with the Differential Die-away Method Within the Scope of the Next Generation Safeguards Initiative Spent Fuel Project," *Journal of Nuclear Materials Management*, Vol. 40, No. *3*, p. 61 (2012).

[5] P.Blanc, H. O. Menlove, S.J. Tobin, S. Croft, and A. Favalli, "An Integrated Delayed-Neutron, Differential Die-Away Instrument to Quantify Plutonium in Spent Nuclear Fuel," *Journal of Nuclear Materials Management*, Vol. 40, No. *3*, p. 70 (2012).

[6] V. Henzl, "How to improve the S/B ratio of the DDA instrument", internal collaboration report, April 2014

[7] V. Henzl, M. T. Swinhoe, and S. J. Tobin: „*Direct Measurement of Initial Enrichment and Burn-Up of Spent Fuel Assembly with a Differential Die-Away Technique Based Instrument"*, Proceedings of the 53rd INMM conference, Orlando, FL, 2012

[8] V. Henzl, private communication

[9] V. Henzl, S. Croft, J. Richard, M. T. Swinhoe, and S. J. Tobin: „*Determination of the Plutonium Content in a Spent Fuel Assembly by Passive and Active Interrogation using a Differential Die-Away Instrument"*, Nucl. Instr. and Meth. A 712, 83-92, 2013